

# Gas permeability tests on concrete damaged by drying shrinkage and its anisotropy effect

N.Burlion

Laboratory of Mechanics of Lille, EUDIL-USTL, Cité Scientifique, 59650 Villeneuve d'Ascq, France

F.Skoczylas

Laboratory of Mechanics of Lille, Ecole Centrale de Lille, Cité Scientifique, 59650 Villeneuve d'Ascq, France

**ABSTRACT:** Concrete structure, used to store radioactive materials, are subjected to mechanical, hydrous and thermal loading, which can affect the structural strength, the porous space and permeability. The knowledge of the behaviour and the main characteristic of the material should be checked in order to take into account drying shrinkage. In the first part, we present the experimental devices and the principal parameters studied. Prismatic samples are used for drying shrinkage and loss of mass during time measurements, and measurements of drying shrinkage. In a second part, gas permeability tests were carried out on this material after approximately 10 months of drying. Samples are cored from each prismatic sample (used for shrinkage measurements) : either from the transverse direction or from the longitudinal direction. Principles of gas permeability test are presented and experimental process is described. Finally, we discuss the experimental results obtained in terms of anisotropy induced by the desiccation phenomenon. As a result, an induced anisotropy of permeability is then measured experimentally.

## 1 INTRODUCTION

This study is concerned with the effects of drying shrinkage and induced damage of concrete material in terms upon its gas permeability. As a consequence of its low cost and its ability to be formed, concrete is widely used even if the ageing process of the material is complex. This process leads to a change in mechanical and hydraulic behaviour, in chemical properties and saturation level. These changes are obviously linked to the material and structure surround. Under drying conditions, the free interstitial water can evaporate. Thus, the cementitious matrix is subjected to tensile stresses, which may induce microcracks if the material tensile strength is exceeded (Bazant and Raftshol 1982, Bazant and Wittmann 1982, Acker 1988). The knowledge of its ageing process and its consequences upon the properties, mentioned above, is crucial for material intended for use in the manufacture of containers for highly radioactive elements. For confining or water retaining structures, permeability is one of the most important property which has been the subject of numerous studies (Wang *et al* 1997, Aldea *et al.* 1999). From an experimental perspective, the degradations in concrete modulus or strength and the corresponding change in water permeability due to static loading and microcracking has been demonstrated and documented in the literature (Samaha and Hover 1992).

Furthermore, one of the main requirement for

concrete containment structure is a low concrete permeability : to prevent the environment from pollution and as this quantity is indicative if the durability of concrete. In the mean time and even if only superficially observable (Acker and Collina 2000, Sadouki and Wittmann 2000), microcracks of the cement paste are induced by drying and desiccation shrinkage. This induced microcracking will lead to an increase in permeability which is generally assumed to be isotropic, especially when drying occurred from heat treatment (Hearn 1999). On the other hand, concrete structures exhibit main drying direction which is often along their lowest size – i.e. – along the highest hydrous gradient. To verify whether the permeability variations are isotropic or not, gas permeability measurements have been carried out on a concrete submitted to natural drying. In these tests, two different permeabilities were measured : in the following highest hydrous gradient direction and the perpendicular one.

This study is divided in two parts. The first part is concerned with the drying process which induces microcracks. The concrete used and its curing conditions are described. To evaluate the direct drying effects, lost in mass and shrinkage measurements are then presented. Mechanical uniaxial tests performed on concrete cylinders at different times are also presented, in order to point out the effect of induced drying microcracking on mechanical properties of concrete. Over a ten months period – the time re-

quired to achieve drying process – two smaller samples are cored from each specimen used for the previously mentioned measurements. The samples are intended for the gas permeability tests that make up the second part of the study. An anisotropic variation of permeability, induced by drying and desiccation shrinkage, can be observed. The main results are described and commented on, with a view to suggest a model intended to simulate drying and damage phenomena in concrete structures.

## 2 MICROFISSURATION DEVELOPMENT : EXPERIMENTAL INVESTIGATION ON DRYING SHRINKAGE

### 2.1 *Material and specimens design*

The total shrinkage of concrete can be decomposed of several parts (Acker 1988, Wittmann 82, Aïtcin *et al.* 1998) and the influence of each part is correlated with the concrete composition (Bazant and Wittmann 1982, de Larrard and Le Roy 1992, Baroghel-Bouny 1994, Baroghel-Bouny *et al.* 1998) : endogenous shrinkage, thermal shrinkage and desiccation shrinkage. Thermal shrinkage is caused by cooling process after the formation of concrete whose temperature increases by effect of cement hydration. Self-desiccation shrinkage is coming from internal material drying by consuming water in pores during hydration process. The endogenous shrinkage is defined as the sum of Le Châtelier contraction and self-desiccation shrinkage (Hua 1992, Granger *et al.* 1994, Bazant 1999, Ulm *et al.* 1999). Finally, the desiccation shrinkage is induced by the disturbance of hydrous equilibrium between the inside body of concrete and its exterior surface. This hydrous gradient causes the leak-off of free water from concrete. Such a change of water content induces a compressive deformation of skeleton material due to increase of capillary pressure. However, this deformation is partially prevented by both gravels and heterogeneous hygrometric states in concrete body. A tensile stress appears in cement matrix. There is initiation and propagation of microcracks when the tensile stress exceeds the material strength. In fact, microcracks would be orientated by drying gradient. In this work, we present a study of the influences of such microcracks on the gas permeability in the same direction of drying, and in the normal direction of drying.

In order to capture this desiccation process and its consequences, it is necessary to design a specific laboratory testing procedure. The choice of concrete material is made in a manner to maximise shrinkage deformation in a relative short time. There is a relationship between drying shrinkage and the ratio W/C (water/cement) (Pihlajavaara 1982, Baroghel-Bouny

*et al.* 1998). We have chosen a concrete with a high value of the ratio W/C. Indeed, such a material presents a high initial permeability facilitating leak-off of water from sample. In addition, a strong shrinkage should be observed in concrete with a small diameter of biggest gravel and a high ratio water/cement. Consequently, we have used a concrete with 8 mm diameter of biggest gravel and a W/C equal to 0.6. The cement is CEMIIb 32.5. The composition of concrete is 324 kg/m<sup>3</sup> for the cement, 205 kg/m<sup>3</sup> for water, 1110 kg/m<sup>3</sup> of gravel 4/8 mm, and 668 kg/m<sup>3</sup> of sand 0/4 mm. The real W/C ratio is then equal to 0.63. This composition is used in order to obtain an uniaxial compression strength less than 30 MPa at 28 days. With this W/C ratio, the cement matrix structure is formed of big diameter pores (Reinhardt 1994, Baroghel-Bouny 1994, Baroghel-Bouny *et al.* 1998) and then allows a high drying kinetics. After 28 days, the cement porous structure is completed (Aïtcin *et al.* 1998), and this lets us to consider that hydric exchange will occur with a quasi constant porosity for each specimen.

The measuring of shrinkage should be made on small size samples. For shrinkage measurement, the size of prismatic specimens is 40x40x160 mm<sup>3</sup>. The self-desiccation shrinkage occurs mainly during hydration (Acker 1988, Hua 1992) and then can be neglected after 28 days. This was confirmed in (Baroghel-Bouny *et al.* 1998) where it was observed that endogenous shrinkage stopped after 28 days while the drying shrinkage continued to progress. Colina and Acker showed that the temperature is stabilised in a one meter size cube after 31 days (Colina and Acker 2000). It is then reasonable to assume that the temperature will become constant in our specimens after 28 days. Consequently, the thermal shrinkage can also be neglected.

The specimens were kept in a pool at a 20°C constant temperature during 28 days. In order to avoid dissolution of portlandite in water, the prismatic specimens were preserved inside plastic bags emerged in water. After 28 days of curing, the specimens were taken off from water and kept under a relative humidity of 60 % ± 5% and a temperature of 21°C ± 1°C.

Furthermore, an asymptotic stabilisation of desiccation shrinkage occurs after 90 days (Pihlajavaara 1974, Baroghel-Bouny *et al.* 1998). This let us to consider that the main shrinkage is produced during the first three months of drying which is a reasonable duration for the proposed study. The scale effect should also be taken into account in the shrinkage phenomenon of concrete (Pihlajavaara 1974, Bazant and Wittmann 1982, Granger *et al.* 1997). Indeed, the internal variation of hydrous states are dependent on sample size. Bigger is the structure size slower are the hydrous state changes. Inversely, there is a rapid variation of water content in struc-

tures with small characteristic size. Accordingly, the effect of drying shrinkage on the mechanical behaviour of concrete may be detectable only in small size structures (Pihlajavaara 1974, Acker 1988). This justifies that the used specimen size is judicious with respect to that we want to show.

2.2 Desiccation shrinkage results : its influence on microcracks

To take into account the cure procedure, the following hypothesis is assumed : when samples are taken out water, they are saturated. The global water content is then deduced from the loss in mass of specimens. Figure 1 shows the evolution of shrinkage strain versus time of drying. Figure 2 shows the evolution of shrinkage strain in three specimens as a function of loss in mass during 70 days of drying. The results are similar to those obtained by Granger (Granger 1994). Two phases can be distinguished. The first part of the curves corresponds to the rapid drying of specimen surface. This arises with superficial microcracking which delays the progress of global shrinkage. In the second phase, there is proportionality between loss in mass and shrinkage strain, this evidences the effect of drying on concrete. If the measurement was continued after 70 days, a third phase would be obtained where the shrinkage strain would tend to stabilise while the loss in mass continues to evolve. Such a phase is of low interest here because in general, no further growth of microcracks is observed during this period.

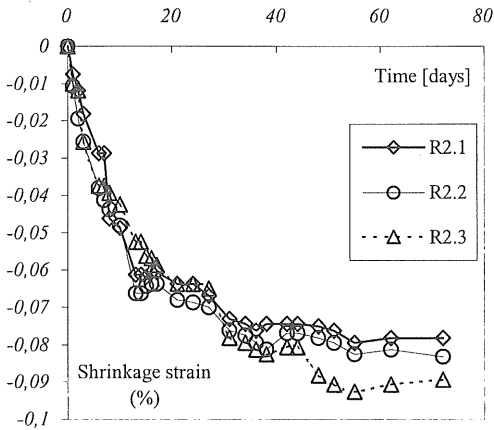


Figure 1 : Evolution of shrinkage strain versus time for 3 prismatic specimens

Uniaxial compression tests were performed on the same concrete at different time of drying. During drying, the water content is no more uniform in the specimen, this leads to the definition of an overall

elastic stiffness of specimen rather than the elastic modulus of concrete material.

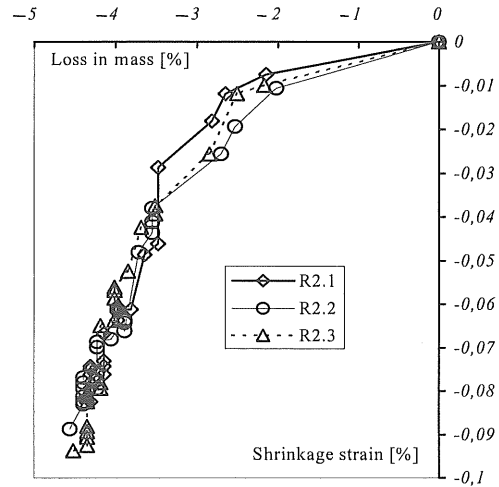


Figure 2 : Evolution of shrinkage versus the loss in mass for 3 prismatic specimens

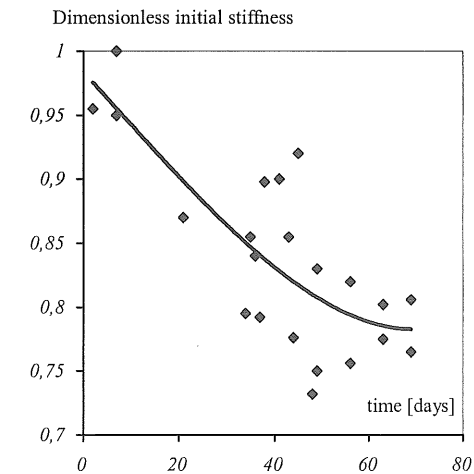


Figure 3 : Evolution of dimensionless initial stiffness versus time of drying

The elastic stiffness is strongly influenced by growth of microcracks during drying shrinkage. In order to compare the results obtained from different specimens, we define the dimensionless initial stiffness, which corresponds to the stiffness measured from the third loading-unloading cycle in each test (the corresponding axial stress is 9 MPa), divided by the maximal value of this initial stiffness obtained in all specimens. Figure 3 shows the evolutions of dimensionless initial stiffness in cylinder specimens (220 mm height, diameter 110 mm) as functions of time of drying. Each point represents the average value of two tests performed the same day. It is clear

that the drying process induces a diminution of elastic stiffness of concrete, thus induces microcracks.

### 2.3 Specimens for permeability measurements

For the determination of the permeability, the mechanical effect induced by the drying shrinkage has to be taken into account. The reason is due to the fact that deformations induced by the hydrous imbalance between the inside and the outside of the material, are prevented which leads to a microcracking of the concrete. This microcracking will thus have an influence on its mechanical behaviour and its permeability. The drying of concrete is directed by the hydrous gradient applied on the sample and the microcracking obtained has also privileged orientation.

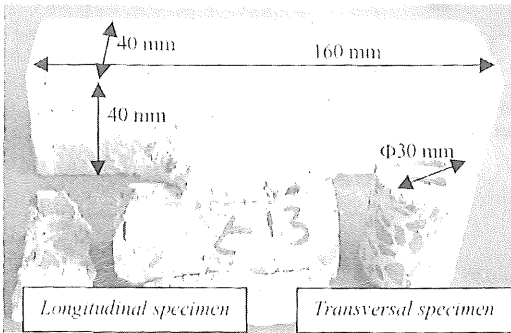


Figure 4 : Photograph of specimens

In order to show up a possible anisotropy of permeability, induced by desiccation process, cylindrical samples, 30 mm diameter, were cored from those used for the previous tests. Before coring, the prismatic samples have been kept under the conditions mentioned before (§ 2.1) for ten months. Those corings are respectively carried out in the longitudinal and transversal sizes of the prismatic sample (figure 4). The 30 mm samples are then stuck into a 66 mm diameter metallic tube, with Araldite® glue (figure 5). This specific preparation allows the sample to be used in the triaxial cell of our laboratory.

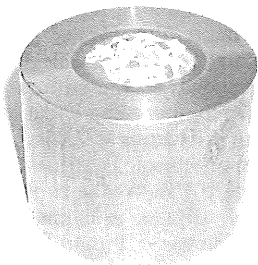


Figure 5 : Photograph of gas permeability specimen

## 3 GAS PERMEABILITY MEASUREMENTS : INFLUENCE OF MICROCRACKING INDUCED BY DRYING

### 3.1 General principles of gas permeability measurements

In the following, we present the experimental method aimed at measuring the gas permeability of the material. The injected gas is argon U of above 99% purity, which will be considered as a perfectly pure gas in the rest of the study. The general principles of testing conditions is to subject the cylindrical sample to a low confining pressure and static gas pressure on its upper and lower surfaces, followed by the application of a slight excess of pressure to one of the sides and to record over a period of time the evolution in the difference of pressure between the two surfaces. This test is similar to a low amplitude pulse test (Skoczylas and Henry 1995). The experimental apparatus used is shown in figure 6.

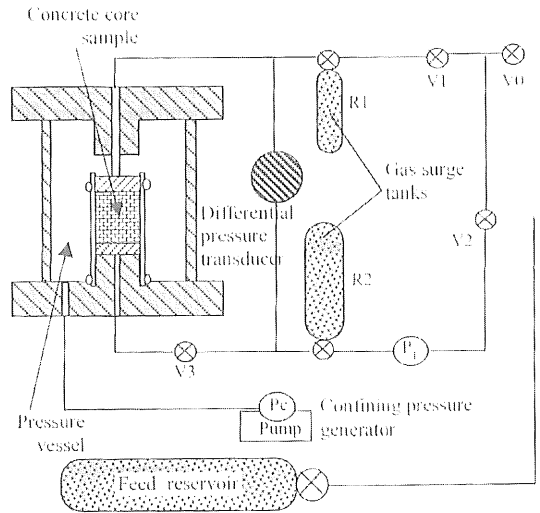


Figure 6 : Diagram showing experiment and equipment.

This assembly comprises:

- A confining cell
- A Gilson® pump and a digital manometer capable of applying the confining pressure
- A gas injection circuit comprising :
  - An argon supply reservoir and a high-pressure reducer manometer.
  - Two surge reservoirs R1 and R2 : the sample is placed between the two.
  - A digital manometer for measuring the static pressure
  - A transmitter and a differential pressure indicator to apply and measure the difference in pressure between both sides of the sample.

- A computer for recording the difference in pressure between both sides of the sample, over a period of time.

### 3.2 Testing boundary conditions

The sample and tube are placed inside the cell and subjected to the confining pressure, fixed at 3 MPa. The static pressure  $P_i = 2$  MPa is then applied to both faces ; the two reservoirs are at the same pressure and are connected by opening valves V1, V2 and V3. After a 3-hour wait, required for balancing the internal pressures, the two injection circuits are isolated by closing valves V1 and V3. A slight excess in injection pressure  $\Delta P_i$  is applied to reservoir R<sub>1</sub> and valve V3 is opened to allow the gas to be diffused over the whole sample. Evolution  $(P_2(t)-P_1(t)) = \Delta P(t)$  can then be measured and read on the differential pressure indicator. We have chosen an excess pressure  $\Delta P_i = 0.02$  MPa. This value lies within the range of generally accepted excess pressures (Walder and Nur 1986, Walls 1982). Figure 7 gives a highly simplified representation of the experiment and will enable us to indicate the boundary conditions for this test.

Boundary conditions are :

- At time  $t < 0$ ,  $P_2 = P_1 = P_i$
- At time  $t=0$ ,  $P_1 = P_i + \Delta P_i$ ,  $P_2 = P_i$
- At time  $t > 0$ ,  $P_1 = P_1(t)$ ,  $P_2 = P_2(t)$
- At final time  $P_2 = P_1 = P_f$

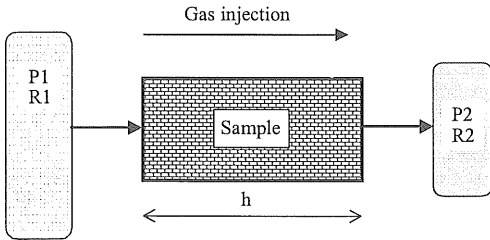


Figure 7 : Experimentation conditions

### 3.3 Hypotheses and data processing

In this study, it is supposed that the fluid flow obeys Darcy's law. The flow is sufficiently slow to be considered as laminar and the static pressure sufficiently high for the Klinkenberg effect (Iffly 1956) to be ignored. In such as case it can be written that:

$$\vec{V} = -\frac{K}{\mu} \overrightarrow{\text{grad}P} \quad (1)$$

$K$  is thus the permeability of the medium to gas, expressed in  $\text{m}^2$ .  $\mu$  is the viscosity of argon. Taking into account the mass balance equation and ignoring the effects of poromechanical coupling on the fluid pressure because of the high level of the latter's

compressibility, the well known diffusivity equation is obtained :

$$\frac{K}{\mu} \text{div}(\overrightarrow{P \text{ grad}P}) = \phi \frac{\partial P}{\partial t} \quad (2)$$

$\phi$  is the porosity of the material which remains free for the circulation of gas .

During the test, the only measurement available are the variations of pressure in the reservoirs  $P_1(t)$  and  $P_2(t)$  and  $\Delta P(t)$ . To find permeability  $K$  using such measurements, two methods can be envisaged : a numerical analysis using, for example, the finite element method (Skoczylas and Henry 1995) or a simplified method, originally described by Brace and Walsh (Brace and Walsh 1968). In this case, we have chosen the latter type of method. The basic hypothesis is that this transient state (pulse-test) is formed of a succession of steady states with the following boundary conditions :

- $P_1 = P_1(t)$  at  $x=0$
- $P_2 = P_2(t)$  at  $x = h$

Since the pulse amplitude is very low compared with the initial static pressure, it can be shown (Dana and Skoczylas 1999), at this stage, that:

$$P_1(t) - P_2(t) = \Delta P(t) = \Delta P_i \exp(-c P_f t) \text{ with}$$

$$c = -\frac{KA}{\mu h} \left( \frac{1}{V_1} + \frac{1}{V_2} \right) \quad (3)$$

This result is used to calculate permeability  $K$  by comparing this theoretical drop in pressure and the real measurement, as well as by choosing coefficient  $c$ , which gives the theoretical value closest to the measured value.

### 3.4 Results in anisotropic permeability measurements

Six permeability measurements were performed on three different samples submitted to a ten months period of drying. As mentioned before, two smallest cylinders were cored from each of these samples along the longitudinal direction and the transversal direction (highest hydrous gradient direction). This allowed two different permeabilities to be measured respectively  $K_L$  (longitudinal permeability) and  $K_T$  (transversal permeability) in order to assess a possible micro-cracking anisotropy and its consequence upon material permeability. The results of measurements are given in table 1 below.

Table 1 : Permeability measurements : results

Sample number	$K_L$ ( $\text{m}^2$ )	$K_T$ ( $\text{m}^2$ )	$K_T / K_L$
2.1	$5 \cdot 10^{-16}$	$5 \cdot 10^{-16}$	1
2.2	$3.9 \cdot 10^{-16}$	$6.8 \cdot 10^{-16}$	1.74
2.3	$2.9 \cdot 10^{-16}$	$3.4 \cdot 10^{-16}$	1.17

As the permeability ranging is measured from 2.9 to  $6.8 \cdot 10^{-16} \text{ m}^2$ , these results show that this property

is almost homogeneous for the tested concrete. Except for sample 2, it can not be observed a significant increase in transversal permeability with respect to longitudinal one. Microcracks are certainly formed but either in insufficient number or with an opening which is too weak for the permeability to increase significantly. This second point has to be underlined and related to experiments previously performed in our laboratory (Meziani and Skoczylas 1999). The aim of these tests was to clarify experimentally the respective roles of mechanical damage (i.e. microcracking) and the degree of microcracks opening on the increase in permeability. The variation of that was continuously recorded under triaxial loading (open cracks) and after unloading (closed cracks). Considerable differences were observed and showed that permeability is highly conditioned by the degree to which the microcracks have opened at a given damage level. As a conclusion, these slight differences in transversal and longitudinal permeabilities have to be confirmed by further tests carried out on older specimens (period of 20 months of drying); these differences could be amplified if the material was subjected to a deviatoric loading (likely to lead to an opening of microcracks).

#### 4 CONCLUSIONS

In this study, we have shown up the influence of desiccation induced microcracking on mechanical properties and gas permeability of concrete. Tests results of drying shrinkage were presented and correlated with stiffness loss of cylindrical concrete specimens submitted to uniaxial compression. An induced microcracking of the material leads to an increase of gas permeability. In a second part, we have pointed out the existence of an induced anisotropy in term of permeability. It traduces the fact that microcracks occur preferentially along the highest drying gradient induced by the structure geometry. Nevertheless, this anisotropy is relatively small when material is unloaded. An experimental investigation of permeability under mechanical load might show an higher anisotropy with the opening of drying induced microcracks. With a point of view of modelling, this first study proves that taking to account an isotropic permeability will give good response in term of drying. Besides, the importance of other parameters on drying of concrete (for instance the sorption – desorption isotherm) minimise the influence of this anisotropic behaviour. This result has to be confirmed by new experimental tests that will be carried out soon on the same concrete after twenty months of drying.

#### REFERENCES

- Acker, P. 1988. Comportement mécanique du béton : apports de l'approche physico-chimique, Phd Thesis of Ecole Nationale des Ponts et Chaussées, Paris, Rapport de Recherche LPC 152.
- Aïtcin, P.C., Neville, A. & Acker, P., 1998. Les différents types de retrait du béton, *Bulletin des Laboratoires des Ponts et Chaussées* 215, ref. 4184, 41-51.
- Aldea, C.-M., Shah, S.P. & Karr, A. 1999. Permeability of cracked concrete, *Materials and Structures* 32, 370-376.
- Bazant, Z.P. 1999. Criteria for rational prediction of creep and shrinkage of concrete', *Revue Française de Génie Civil* 3(3-4), 61-89.
- Bazant Z.P. & Raftshol W.J. 1982. Effect of cracking in drying and shrinkage specimens, *Cement and Concrete Research* 12, 209-226.
- Bazant, Z.P. & Wittmann, F.H. 1982. *Creep and Shrinkage in Concrete Structures*, J. Wiley and Sons.
- Baroghel-Bouny, V. 1994. Caractérisation microstructurale et hydrique des pâtes de ciment et des bétons ordinaires et à très hautes performances, Phd Thesis of Ecole Nationale des Ponts et Chaussées, Paris.
- Baroghel-Bouny, V, Rougeau, P., Care, S. & Gawsewitch, J. 1998. Etude comparative de la durabilité des bétons B30 et B80. I- Microstructure, propriétés de durabilité et retrait, *Bulletin de Liaison des Laboratoires des Ponts-et-Chaussées* 217, réf. 4204, 61-73.
- Brace, W. F. & Walsh, W. T. 1968. Permeability of granite under high pressure, *Journal of Geophysical Research*, 73(6), 2225-2236.
- Burlion, N., Bourgeois, F. & Shao, J.F. 2000. Coupling damage –drying shrinkage : experimental study and modelling, Proceedings of the Int. RILEM Workshop on *Shrinkage of Concrete, Shrinkage 2000*, Ed. by V. Baroghel-Bouny and P.-C. Aïtcin, Paris, October 16-17.
- Colina, H. & Acker, P. 2000. Drying cracks : Kinematics and scale laws, *Materials and Structures* 33, 101-107.
- Dana, E. & Skoczylas, F. 1999. Gas relative permeability and pore structure of sandstones, *International Journal of Rock Mechanics and Mining Sciences*, 36 (5), 613-625.
- de Larrard, F. & Le Roy, R. 1992. Relation entre formulation et quelques propriétés mécaniques des bétons à hautes performances, *Materials and Structures* 25, 464-475.
- Granger, L. 1994. Comportement différé du béton dans les enceintes de centrales nucléaires : Analyse et modélisation, Phd Thesis of Ecole Nationale des Ponts et Chaussées, Paris.
- Granger L., Torrenti, J.M. & Diruy, M. 1994. Simulation numérique du retrait du béton sous hygrométrie variable, *Bulletin de Liaison des Laboratoires des Ponts-et-Chaussées* 190, réf. 3811, 57-64.
- Granger, L., Torrenti, J.M., & Acker, P. 1997. Thoughts about drying shrinkage : Scale effects and modelling, *Materials and Structures* 30, 96-105
- Hearn, N. 1999. Effect of shrinkage and load-induced cracking on water permeability of concrete, *ACI Materials Journal* 96(2), 234-241.
- Hua, C. 1992. Analyses et modélisations du retrait d'autodesiccation de la pâte de ciment durcissante, Phd Thesis of Ecole Nationale des Ponts et Chaussées, Paris.
- Iffly, R. 1956. Etude de l'écoulement des gaz dans les milieux poreux (in French), *Rev. de l'I.F.P.*, 11(6), 757-796.
- Meziani, H. & Skoczylas, F. 1999. An experimental study of the mechanical behaviour of a mortar and its permeability under deviatoric loading, *Materials and Structures* 32, 403-409.
- Pihlajavaara, S.E. 1974. A review of some of the main results of a research on the ageing phenomena of concrete, effect

- of moisture conditions on strength, shrinkage and creep of mature concrete, *Cement and Concrete Research* 4.
- Pihlajavaara, S.E. 1982. Estimation of drying of concrete at different relative humidities and temperatures of ambient air with special discussion about fundamental features of drying and shrinkage, *Creep and Shrinkage in Concrete Structures*, edited by Z.P. Bazant and F.H. Wittmann, J. Wiley and Sons, 87-108.
- Reinhardt, H.W. 1994. Relation between the microstructure and structural performance of concrete, Proceedings of the Int. RILEM Workshop on *Technology Transfer on the New Trend in Concrete*, Edited by A. Aguado, R. Gettu, S. Shah, ConTech'94, Barcelona, 19-32.
- Samaha, H.R. & Hover, K.C. 1992. Influence of microcracking on the mass transport properties of concrete, *ACI Materials Journal* 89(4), 416-424.
- Sadouki, H. & Wittmann, F.H. 2000. Shrinkage and internal damage induced by drying and endogeneous drying, Proc. of the Int. RILEM Workshop on *Shrinkage of Concrete, Shrinkage 2000*, Ed. by V. Baroghel-Bouny and P.-C. Aït-cin, Paris, October 16-17.
- Skoczylas, F. & Henry, J. P. 1995. A study of intrinsic permeability to gas, *Int. J. Rock Mech. Min. Sci. & Geomech. Abstr.*, 32(2), 171-179.
- Ulm, F. J., Le Maou F. & Boulay C. 1999. Creep and shrinkage coupling : New review of some evidence, *Revue Française de Génie Civil* 3(3-4), 21-37.
- Walder, J. & Nur, A. 1986. Permeability measurement by the pulse-decay method: Effect of poroelastic phenomena and non-linear pore pressure diffusion, *Int. J. Rock Mech. Min. Sci. & Geomech. Abstr.*, 23(3), 225-232.
- Walls, J. D. 1982. Effects of pore pressure, confining pressure and partial saturation on permeability of sandstones, Ph.D. Thesis, Stanford University.
- Wang, K., Jansen D., Shah S.P. & Karr A. 1997. Permeability study of cracked concrete, *Cement and Concrete Research* 27(3), (1997).
- Wittmann, F.H. 1982. Creep and shrinkage mechanisms, *Creep and Shrinkage in Concrete Structures*, edited by Z.P. Bazant and F.H. Wittmann, J. Wiley and Sons, (1982), 129-161.